© 2017. Published by The Company of Biologists Ltd | Development (2017) 144, 1687-1697 doi:10.1242/dev.144261

RESEARCH ARTICLE

Glutathione peroxidase 4 inhibits Wnt/β-catenin signaling and regulates dorsal organizer formation in zebrafish embryos

Xiaozhi Rong[1,2,3,4], Yumei Zhou[1], Yunzhang Liu[1], Beibei Zhao[1], Bo Wang[1], Caixia Wang[1], Xiaoxia Gong[1], Peipei Tang[1], Ling Lu[1], Yun Li[1], Chengtian Zhao[2,3] and Jianfeng Zhou[1,4,*]

ABSTRACT

The Wnt/β-catenin signaling pathway plays pivotal roles in axis formation during embryogenesis and in adult tissue homeostasis. Glutathione peroxidase 4 (GPX4) is a selenoenzyme and participates in the reduction of peroxides. Its synthesis depends on the availability of the element selenium. However, the roles of GPX4 in vertebrate embryonic development and underlying mechanisms are largely unknown. Here, we show that maternal loss of zebrafish *gpx4b* promotes embryonic dorsal organizer formation, whereas overexpression of *gpx4b* inhibits the development of the dorsal organizer. Depletion of human *GPX4* and zebrafish *gpx4b* (*GPX4*/*gpx4b*) increases, while *GPX4*/*gpx4b* overexpression decreases, Wnt/β-catenin signaling *in vivo* and *in vitro*. Functional and epistatic studies showed that GPX4 functions at the Tcf/Lef level, independently of selenocysteine activation. Mechanistically, GPX4 interacts with Tcf/Lefs and inhibits Wnt activity by preventing the binding of Tcf/Lefs to the promoters of Wnt target genes, resulting in inhibitory action in the presence of Wnt/β-catenin signaling. Our findings unravel GPX4 as a suppressor of Wnt/β-catenin signals, suggesting a possible relationship between the Wnt/β-catenin pathway and selenium via the association of Tcf/Lef family proteins with GPX4.

KEY WORDS: Glutathione peroxidase 4, Wnt/β-catenin signaling, Tcf/Lef, Zebrafish, Dorsal organizer

INTRODUCTION

Animal development and adult tissue homeostasis are controlled by a wide range of molecules. Among these, the Wnt/β-catenin pathway, which is evolutionarily conserved among vertebrates, plays key roles (Clevers and Nusse, 2012; MacDonald et al., 2009). Misregulation of Wnt/β-catenin signaling has been implicated in birth defects, tumorigenesis and other diseases (Anastas and Moon, 2013; Clevers and Nusse, 2012; MacDonald et al., 2009). In the presence of Wnt ligands, the Wnt signal inhibits the degradation of β-catenin (Clevers and Nusse, 2012; MacDonald et al., 2009; Stamos and Weis, 2013). Stabilized β-catenin translocates to the nucleus where it binds to transcription factors of the Tcf/Lef family, leading to the transcriptional activation of Wnt target genes (Cadigan and Waterman, 2012; Clevers and Nusse, 2012; MacDonald et al., 2009). In the absence of Wnt ligands, β-catenin is phosphorylated and targeted by a destruction complex for proteasomal degradation, and Tcf/Lef proteins interact with Groucho transcriptional repressors, preventing gene transcription (Cadigan and Waterman, 2012; Clevers and Nusse, 2012; MacDonald et al., 2009). Thus, in the Wnt/β-catenin pathway, Tcf/Lefs are the key molecules converting transcriptional repressors into transcriptional activators of Wnt target genes upon stimulation of Wnt signals.

Wnt/β-catenin signaling is crucially involved in the axial patterning in vertebrate embryogenesis (Hikasa and Sokol, 2013; Langdon and Mullins, 2011; Petersen and Reddien, 2009). In zebrafish embryos, maternal Wnt/β-catenin signaling promotes the dorsal organizer formation before gastrulation (Bellipanni et al., 2006; Schneider et al., 1996). By contrast, zygotic Wnt/β-catenin signaling promotes ventrolateral mesodermal development to limit the organizer after the onset of gastrulation, and thereafter promotes posterior neural development (Baker et al., 2010; Erter et al., 2001; Lekven et al., 2001; Ramel et al., 2005).

Glutathione peroxidase 4 (GPX4) is a monomeric selenoenzyme harboring a selenocysteine (Sec) in the catalytically active center (Brigelius-Flohe and Maiorino, 2013). Sec, the 21st amino acid, incorporates selenium in selenoproteins in response to the opal UGA codon (Hatfield et al., 2014). Therefore, the element selenium is essential for selenoproteins. Sec efficiently reduces hydroperoxides at the expense of glutathione or other low molecular weight thiol-containing compounds (Hatfield et al., 2014). Thus, GPX4 plays an important role in controlling the cellular redox status (Brigelius-Flohe and Maiorino, 2013). In addition, GPX4 has been found to control 'ferroptosis', a novel nonapoptotic form of cell death involving lipid reactive oxygen species (ROS) (Dixon et al., 2012; Friedmann Angeli et al., 2014; Seiler et al., 2008; Yang et al., 2014). GPX4 is highly conserved in vertebrates from fish to mammals. Previous studies have reported that Sec activation of GPX4 is crucial for survival in mice, and depletion of GPX4 or genetically inactive Sec in mice leads to embryonic lethality around embryonic day 7.5 (Imai et al., 2003; Ingold et al., 2015; Yant et al., 2003). However, besides the reported cellular function and developmental roles in mice, the role of GPX4 in vertebrate embryogenesis and its underlying molecular mechanisms are still poorly understood.

In this study, we used the zebrafish model to investigate the role of GPX4 in early development by using both the CRISPR/Cas9 knockout system and antisense morpholino (MO) knockdown technology. Unexpectedly, maternal loss of zebrafish *gpx4b* and knockdown of *gpx4b* led to dorsal organizer formation deficiency, and GPX4 inhibited the Wnt/β-catenin signaling pathway. We

[1]Key Laboratory of Marine Drugs (Ocean University of China), Chinese Ministry of Education, and School of Medicine and Pharmacy, Ocean University of China, 5 Yushan Road, Qingdao 266003, China. [2]Institute of Evolution and Marine Biodiversity and College of Marine Biology, Ocean University of China, 5 Yushan Road, Qingdao 266003, China. [3]Laboratory for Marine Biology and Biotechnology, Qingdao National Laboratory for Marine Science and Technology, Qingdao 266003, China. [4]Laboratory for Marine Drugs and Biological Products, Qingdao National Laboratory for Marine Science and Technology, Qingdao 266003, China.

*Author for correspondence (jfzhou@ouc.edu.cn)

Y.Z., 0000-0001-9647-6369; B.Z., 0000-0002-2922-4628; X.G., 0000-0001-5481-880X; P.T., 0000-0002-1535-3971; J.Z., 0000-0001-5702-6664

Received 31 August 2016; Accepted 7 March 2017

Development (2017) 144, 1687-1697 doi:10.1242/dev.144261

found that GPX4 interacts with Tcf/Lefs and occupies the Wnt target gene promoters to suppress transcription by preventing the association between Tcf/Lefs and Wnt target gene promoters, resulting in reduced Wnt activity in the presence of Wnt signals. To our knowledge, this is the first report on the cellular function of GPX4 as a repressor of Wnt/β-catenin signaling and on the crucial role of maternally deposited Gpx4b in the regulation of dorsal organizer formation during zebrafish embryogenesis. Importantly, our results also suggest that the Wnt/β-catenin pathway might be modulated by selenium, which, in the form of Sec, is indispensable for cellular synthesis of GPX4.

RESULTS

Maternal loss of zebrafish *gpx4b* impairs dorsal organizer formation and depletion of Gpx4b increases Wnt/β-catenin activity

The zebrafish genome harbors two *gpx4* genes: *gpx4a* and *gpx4b*. Both Gpx4a and Gpx4b contain a Sec site (Fig. S1A). RT-PCR and whole-mount *in situ* hybridization (WISH) with a *gpx4b* antisense probe indicated that the *gpx4b* transcript is maternally deposited and is ubiquitously expressed before 24 h post fertilization (hpf) (Fig. S1B,C) (Mendieta-Serrano et al., 2015; Thisse et al., 2003). Unlike *gpx4b*, previous studies have indicated that *gpx4a* shows zygotic gene expression in the periderm covering the yolk cell only (Mendieta-Serrano et al., 2015; Thisse et al., 2003). Interestingly, recent work has shown that from the 128-cell to 512-cell stages, nuclear Gpx4 expression increased gradually (Mendieta-Serrano et al., 2015). The ubiquitous and dynamic expression of Gpx4 implies that Gpx4 may play an important role in the regulation of embryonic development.

To investigate the role of *gpx4b*, we generated two lines of *gpx4b*-null mutants with non-overlapping 4 bp and 10 bp deletions in the third exon by using the CRISPR/Cas9 system (Fig. 1A-C) (Chang et al., 2013). The mutations cause a frameshift early in the protein-coding region leading to early termination of translation (Fig. 1B). Zygotic mutant fish were viable, morphologically normal and fertile. However, both lines of maternal (M) mutants showed dorsalized phenotypes with reduced ventral tail fins at 26 hpf, although the allele penetrance and expressivity in the 4 bp deletion line appeared to be higher (Fig. 1D). These dorsalized phenotypes are characteristic of weakly dorsalized phenotypes, reminiscent of *mini fin* (*mfn*) and *lost-a-fin* (*laf*) mutant embryos at this stage (Mullins et al., 1996). Unlike the M mutants, all observed embryos from the two lines of maternal-zygotic (MZ) mutants were morphologically normal at 24 hpf (Fig. 1D). As an independent and complementary approach, a translation-blocking *gpx4b* MO was used to inhibit translation of both maternal and zygotic mRNAs. The effectiveness of the MO was confirmed by blocking the translation of a *gpx4b* 5′-UTR-GFP reporter (Fig. S2A). The specificity of the MO was confirmed by the lack of additional phenotypes in the MZ mutant background. Additionally, as shown in Fig. S2B, we generated a Gpx4b expression vector that contains the ORF and the whole 3′-UTR, including the Sec insertion sequence element to allow insertion of Sec in response to the UGA codon instead of termination of translation (Berry et al., 1991). The expression of Gpx4b was confirmed prior to rescue experiments using *in vitro* transcribed *gpx4b* mRNA (Fig. S2B). Injection of the MO caused relatively stronger dorsalized phenotypes with reduced trunk, a thinner and curved tail, and reduced yolk extension at 26 hpf, which resembled the previously reported *somitabun* (*sbn*) and *swirl* (*swr*) mutants at this stage (Fig. S2C,D) (Mullins et al., 1996). The dorsalized phenotype could be neutralized by co-injection of 50 pg *gpx4b* mRNA, suggesting that the MO specifically targeted *gpx4b* (Fig. S2D). Similarly, co-injection of 50 pg *gpx4a* mRNA rescued the dorsalizing effect caused by the *gpx4b* MO, suggesting that Gpx4a and Gpx4b have comparable ventralizing action (Fig. S2E). Recent studies reported that zebrafish can activate a compensation mechanism, resulting in a mild phenotype, in genetic mutants but not in morphants (Hu et al., 2016; Rossi et al., 2015). To evaluate the discrepancy between the phenotypes observed in mutants and morphants, we carried out quantitative real-time reverse transcription PCR (qRT-PCR) analysis of *gpx4a* and *gpx4b* at different developmental stages. The transcript levels of *gpx4b* were not decreased in M and MZ mutants at 4 hpf but were significantly decreased in MZ mutants at 6 hpf and 9 hpf, indicating a gradually increasing *gpx4b* mRNA degradation rate (Fig. S2F). Meanwhile, the *gpx4a* mRNA levels were significantly elevated (Fig. S2F). In *gpx4b*-knockdown morphants, the expression of *gpx4b* was not reduced nor was *gpx4a* upregulated when compared with cMO-injected embryos (Fig. S2F). Collectively, these data suggested that Gpx4a probably functions as a compensating protein in *gpx4b* mutants.

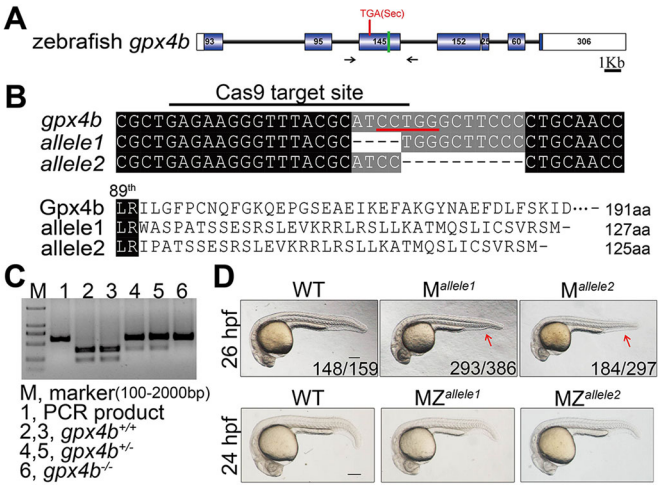

Fig. 1. Generation of the *gpx4b* mutant using the CRISPR/Cas9 system, and the gross phenotypes of maternal and maternal-zygotic loss of *gpx4b* in zebrafish embryos. (A) Schematic representation of the *gpx4b* locus. Exons are shown as boxes (filled box, protein-coding region; open box, UTR). Introns are shown as lines. The location of the Sec codon, TGA, is indicated with a red line. The green line indicates the location of the Cas9 target site. Black arrows show the position of genotyping primers. (B) The sequence of Cas9 target site and predicted protein sequences of wild type (WT) and mutant *gpx4b* alleles (allele1 and allele2). Upper panel: the sequence of the Cas9 target site is indicated with a black line and the two *gpx4b*-null mutant alleles are shown. The black dashed line indicates a deletion. Red line, restriction enzyme *Bci*T1301 recognition sequence. Lower panel: the protein sequences of wild type and mutants are shown. (C) Genotyping result using restriction enzyme *Bci*T1301 digestion assay. (D) Representative views of wild type as well as maternal (M) and maternal-zygotic (MZ) mutants of *gpx4b* at the indicated stages. The arrow shows the reduced ventral tail fin. The frequency of embryos with the indicated patterns is shown in the bottom right corner of each panel. *n*=4 females for allele1, *n*=3 females for allele2. At least two clutches of embryos from each female were analyzed. Lateral views with anterior towards the left. Scale bar: 200 µm.

In zebrafish, maternal and zygotic Wnt/β-catenin appears to have different effects on dorsoventral patterning formation (Hikasa and Sokol, 2013; Langdon and Mullins, 2011; Petersen and Reddien, 2009). The phenotypic differences between M and MZ mutants, as well as morphants, prompted us to investigate whether or not dorsal organizer formation was impaired and Wnt/β-catenin signaling

Development (2017) 144, 1687-1697 doi:10.1242/dev.144261

abrogated. To characterize the consequences of loss of Gpx4b on embryonic patterning, we examined the expression of a suite of region-specific marker genes at different developmental stages. In both the M and MZ mutant lines of *gpx4b*, expression of the organizer-specific markers *chordin* (*chd*) and *goosecoid* (*gsc*) was laterally and ventrally expanded at 4.3 hpf, as indicated by whole-mount *in situ* hybridization (Fig. 2A,B and Fig. S3A,B). Similarly, the *gpx4b*-knockdown embryos showed broad expansion of *chd* and *gsc* expression at 4.3 hpf (Fig. S3C,D). At shield stage (6 hpf), the expression domains of *chd* and *gsc* were also laterally and ventrally expanded in M mutants (Fig. S3E,G). Another, maternal mutant allele1 showed a higher ratio of embryos with expanded expression of organizer markers at 4.3 hpf and 6 hpf, which was consistent with the higher penetrance of allele1 at 26 hpf (Fig. 2A,B and Fig. S3A,B,E,G). Conversely, the ventrally restricted markers *even-skipped-1* (*eve1*), *bmp4*, *bmp2b* and *sizzled* (*szl*) exhibited reduced expression domains at 6 hpf (Fig. S3F,G). Similar dorsoventral patterning was observed in the *gpx4b*-knockdown embryos (Fig. S3H,I). Unlike M mutants and *gpx4b*-knockdown morphants, however, the expression domains of the dorsoventral marker genes returned to the control levels in MZ mutants in comparison with wild type (Fig. S3E-G). Next, we investigated the role of Gpx4b in anteroposterior neural patterning. The expression of the forebrain marker *six3b*, the midbrain-hindbrain boundary marker *pax2a* and the hindbrain marker *krox20* (*egr2b* – Zebrafish Information Network) was used to assess the anteroposterior neural patterning. As shown in Fig. S3J, the anteroposterior neural patterning was not affected in *gpx4b* MZ mutant embryos at 12.5 hpf. Taken together, these results indicated that absence of maternal Gpx4b promotes dorsal development before the onset of gastrulation, whereas loss of both maternal and zygotic Gpx4b has little effect on dorsoventral patterning and anteroposterior neural patterning in the zebrafish gastrula.

The effect of loss of *gpx4b* on the Wnt/β-catenin signaling pathway was investigated next. As *chd* and *gsc* are main targets of maternal Wnt at 4.3 hpf, we speculated that Gpx4b may act as an inhibitor of the Wnt/β-catenin signaling pathway. To test this hypothesis, we investigated the expression of direct Wnt target genes at different developmental stages. At 4.3 hpf, the expression of three targets of maternal β-catenin, *boz* (*dharma* – Zebrafish Information Network), *chd* and *squint* (*sqt*) (*ndr1* – Zebrafish Information Network) was significantly upregulated in both M and MZ mutants, as determined by qRT-PCR (Fig. 2C, Fig. S4A). Additionally, the expression areas of three direct target genes of zygotic Wnt, *cdx4*, *sp5l* and *tbx6*, were broadly expanded in MZ mutants, and those of *cdx4* and *sp5l* were also expanded in morphants at the 80-90% epiboly stage (9 hpf), as accessed by whole-mount *in situ* hybridization (Fig. 2D, Fig. S4B,C). Similarly, at the 75% epiboly stage (8 hpf), the expression levels of the direct zygotic Wnt targets *sp5l*, *cdx4*, *ccnd1*, *axin2* and *vent* were significantly increased in MZ mutants, as indicated by qRT-PCR (Fig. 2E and Fig. S4D). We used a well-established Wnt reporter construct TOPFlash to examine the role of endogenous Gpx4b further. Injection of MZ mutants with TOPFlash alone or of wild-type embryos with *gpx4b*-MO resulted in significantly increased Wnt reporter activity (Fig. 2F, Fig. S4E). Taken together, these results suggested that maternal loss of zebrafish *gpx4b* promotes dorsal organizer formation and that depletion of Gpx4b increases Wnt/β-catenin activity.

To further substantiate the developmental role of Gpx4b, we next performed a series of analyses on the progeny of the homozygous females crossed to heterozygous males. The

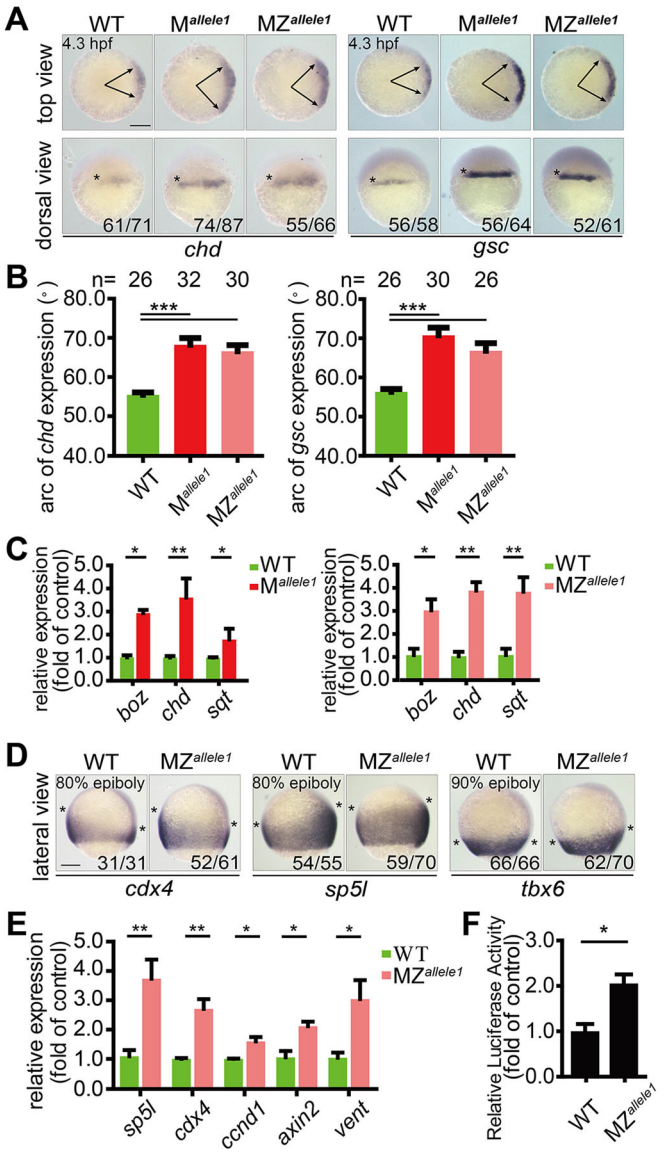

Fig. 2. Maternal loss of *gpx4b* promotes dorsal organizer development and depletion of *gpx4b* increases Wnt/β-catenin activity. (A) Expression of dorsal organizer markers *chd* and *gsc* mRNA in each indicated group of embryos at 4.3 hpf, as assessed by whole-mount *in situ* hybridization. Upper panels are animal pole views with dorsal towards the right. Arrows indicate the edges of the *chd* and *gsc* mRNA expression domains. Lower panels are dorsal views with animal pole upwards. The frequency of embryos with the indicated patterns is shown in the bottom right corner of each group. (B) Quantification of the arc of marker expression shown in A. (C) The expression levels of *boz*, *chd* and *sqt* mRNA in each indicated group of embryos at 4.3 hpf, as analyzed by qRT-PCR. (D) Expression of direct zygotic Wnt markers *cdx4*, *sp5l* and *tbx6* in MZ^{allele1} mutants and wild-type embryos at 80% or 90% epiboly stage (9 hpf). Asterisks indicate the edges of the indicated mRNA expression domains. Lateral views with dorsal towards the right and animal pole upwards. (E) The mRNA expression levels of indicated zygotic Wnt direct target genes in wild-type and MZ^{allele1} mutant embryos at 8 hpf analyzed by qRT-PCR. (F) MZ^{allele1} mutants show increased endogenous Wnt signaling. Values are means± s.e.m. (*n*=3). **P*<0.05; ***P*<0.01; ****P*<0.001. Unpaired *t*-test, two-tailed. Scale bars: 200 µm.

individual embryos were then genotyped to determine whether phenotypes were correlated with genotype or not. As shown in Fig. S5A,B, the expression areas of *gsc* and *eve1* at 6 hpf are correlated with genotypes. Similar results were obtained in the

Development (2017) 144, 1687-1697 doi:10.1242/dev.144261

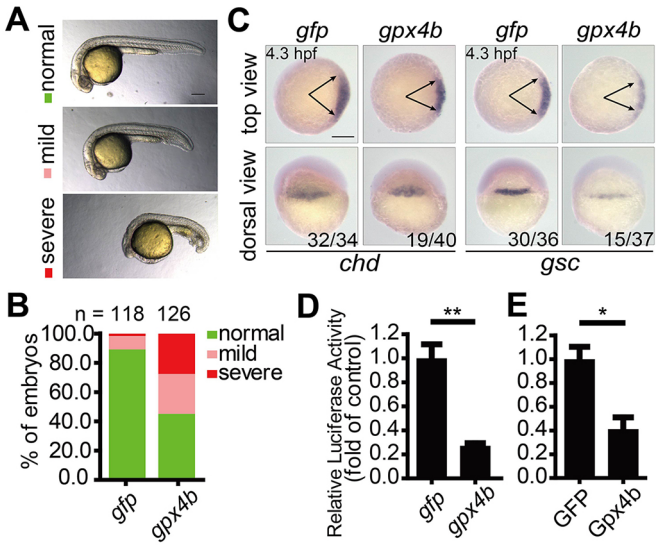

Fig. 3. Overexpression of *gpx4b* ventralizes zebrafish embryos and inhibits Wnt activity. (A) Classification of phenotypes at 24 hpf caused by forced expression of 600 pg *gpx4b* mRNA. (B) Percentage of embryos in each category as shown in A. Results are from three independent experiments and the total embryo numbers are given at the top. (C) Expression patterns of *chd* and *gsc* marker genes in embryos injected with 600 pg *gfp* or *gpx4b* mRNA at 4.3 hpf. The frequency of embryos with the indicated phenotypes is shown in the bottom right corner of each group. (D) Overexpression of Gpx4b inhibits endogenous Wnt signaling *in vivo*. Embryos were injected with TOPFlash reporter DNA with 600 pg *gfp* or *gpx4b* mRNA. (E) Gpx4b inhibits endogenous Wnt signaling *in vitro*. HEK293T cells were transfected with 600 ng GFP plasmid DNA or Gpx4b plasmid DNA together with TOPFlash reporter DNA. Values are means±s.e.m. (n=3). *P<0.05; **P<0.01. Unpaired t-test, two-tailed. Scale bars: 200 µm.

expression area of *cdx4* at 80% epiboly and phenotypes at 26 hpf (Fig. S5C-F). Owing to variable penetrance and expressivity between the two alleles, the allele2 homozygous females were crossed to allele1 heterozygous males. As shown in Fig. S5G,H, the dorsalized phenotype was confirmed by genotyping. Collectively, these data strongly suggest that maternal loss of zebrafish *gpx4b* promotes dorsal organizer formation and that depletion of Gpx4b increases Wnt/β-catenin activity.

Overexpression of *gpx4b* ventralizes zebrafish embryos and inhibits Wnt/β-catenin activity

Next, we investigated the effect of forced expression of *gpx4b*. Injection of 600 pg *gpx4b* mRNA resulted in a ventralized phenotype with reduced head and enlarged ventral tail fin at 24 hpf (Fig. 3A,B). We speculated that these phenotypes may have resulted from the inhibition of maternal Wnt/β-catenin action. Therefore, we further examined the effect of *gpx4b* overexpression on dorsal development at 4.3 hpf. As shown in Fig. 3C, embryos injected with *gpx4b* mRNA consistently showed markedly reduced *chd* and *gsc* expression, indicating the ventralizing effect of Gpx4b before gastrulation. To determine whether Wnt signaling is affected by Gpx4b overexpression *in vivo*, we measured the Wnt reporter activity in *gpx4b* mRNA-injected zebrafish embryos. Forced expression of *gpx4b* mRNA inhibited endogenous Wnt signaling activity in zebrafish embryos (Fig. 3D). Similarly, transfection of Gpx4b into human embryonic kidney (HEK) 293T cells decreased basal Wnt reporter activity (Fig. 3E). These data indicated that Gpx4b negatively regulates Wnt signaling both *in vivo* and *in vitro*.

Inhibitory effect of GPX4 on Wnt/β-catenin signaling is evolutionarily conserved between human and zebrafish

Zebrafish Gpx4b shows a high degree of sequence identity with its human homolog GPX4 (Fig. S1A). This prompted us to explore whether the inhibitory effect of GPX4 on Wnt/β-catenin signaling is conserved in humans. When human *GPX4* was overexpressed in zebrafish embryos, it exhibited a similar ventralizing action in embryos to zebrafish Gpx4b (Fig. 4A,B). We next took a loss-of-function approach to examine whether GPX4 inhibits Wnt/β-catenin signaling in HEK293T cells. To achieve this, a cell line stably expressing GPX4 shRNA was established. The knockdown efficiency was determined by western blot analysis (Fig. 4C). GPX4 knockdown significantly increased endogenous Wnt reporter activity (Fig. 4D). In addition, it resulted in significantly upregulated expression of the direct Wnt target genes such as *MYC*, *CCND1*, *AXIN2*, *DKK1*, *LEF1*, *CDK2* and *CDK5* as indicated by qRT-PCR (Fig. 4E). Collectively, these data suggested that both human GPX4 and zebrafish Gpx4b inhibit Wnt/β-catenin signaling.

GPX4 and Gpx4b inhibit Wnt/β-catenin signaling at the transcriptional level

We then investigated the genetic interaction between GPX4 and Wnt/β-catenin signals in zebrafish embryos and HEK293T cells. Wnt/β-catenin signals consist of multiple proteins, including Wnt ligands, β-catenin and Tcf/Lef proteins. Injection of mRNA for Wnt3a, constitutively active β-catenin (β-CatΔN) or constitutively active Tcf3 (VP16-Tcf3ΔN, β-catenin-independent VP16-Tcf3 fusion protein that lacks the β-catenin-binding site) in zebrafish embryos resulted in an obviously dorsalized phenotype at 12.5 hpf (Fig. 5A,B). Co-injection of *gpx4b* mRNA rescued the dorsalization induced by Wnt3a, β-CatΔN and VP16-Tcf3ΔN in zebrafish embryos (Fig. 5A,B). Similarly, Gpx4b inhibited Wnt reporter activity induced by Wnt3a, β-CatΔN and VP16-Tcf3ΔN in zebrafish embryos (Fig. 5C). Conversely, loss of maternal *gpx4b* synergistically enhanced *β-catΔN-* and *vp16-tcf3ΔN-*induced expression of *boz*, *chd* and *sqt* at 4.3 hpf, as indicated by qRT-PCR analysis (Fig. 5D). Likewise, in HEK293T cells, GPX4 knockdown synergistically enhanced Wnt3a- and VP16-Tcf3ΔN-induced Wnt reporter activity (Fig. 5E,F). Collectively, these data implied that GPX4 and Gpx4b inhibit Wnt/β-catenin signaling at the level of Tcf/Lef.

The GPX4 Sec active site residue is dispensable for Wnt signaling inhibition

The Sec forms the active center of the GPX4 selenoenzyme for hydroperoxide reduction. To test whether or not it is required for Wnt signaling inhibition, we generated Sec-to-Cys mutants ($GPX4^{U73C}$ and $Gpx4b^{U67C}$) and a deletion mutant Gpx4b-C, which lacks both the N-terminal and the Sec site. Like wild-type Gpx4b, $Gpx4b^{U67C}$ inhibited endogenous Wnt reporter activity in HEK293T cells (Fig. 6A). Additionally, consistent with wild-type GPX4 and Gpx4b, both $Gpx4b^{U67C}$ and $GPX4^{U73C}$ ventralized zebrafish embryos (Fig. 6B,C). Similarly, Gpx4b-C inhibited endogenous Wnt reporter activity in HEK293T cells (Fig. 6D). In addition, Gpx4b-C was sufficient to inhibit the Wnt3a- and β-CatΔN-induced Wnt reporter activity in HEK293T cells, as well as to neutralize their dorsalizing activity in zebrafish embryos (Fig. 6E,F). Taken together, these results indicated that the Sec residue is dispensable for Wnt signaling inhibition.

Development (2017) 144, 1687-1697 doi:10.1242/dev.144261

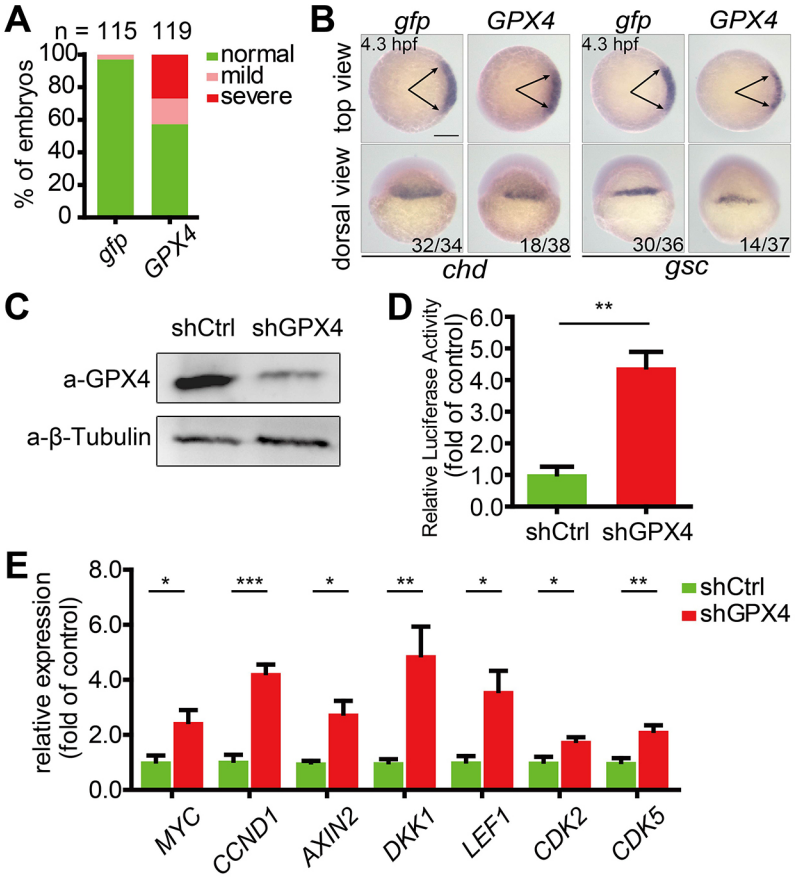

Fig. 4. Wnt inhibitory activity is evolutionarily conserved between zebrafish Gpx4b and human GPX4. (A) The phenotypes of embryos injected with 600 pg *gfp* or *GPX4* mRNA were scored and presented following the criteria described in Fig. 3A. Results are from three independent experiments and the total embryo numbers are given at the top. (B) Human GPX4 alters the expression of *chd* and *gsc* in zebrafish embryos at 4.3 hpf. Embryos injected with 600 pg *gfp* or *GPX4* mRNA were analyzed by whole-mount *in situ* hybridization. The frequency of embryos with the indicated phenotypes is shown in the bottom right corner of each group. (C) Effectiveness of GPX4 shRNA at the protein level in HEK293T cells. shCtrl, control shRNA; β-tubulin, internal control. (D) Knockdown of *GPX4* enhances endogenous Wnt signaling *in vitro*. The stable control or *GPX4* knockdown lines were transfected with TOPFlash reporter DNA. (E) Stable knockdown of *GPX4* in HEK293T cells increased the expression of the indicated Wnt direct target genes. Expression levels were analyzed by qRT-PCR. Values are means±s.e.m. (n=3). *P<0.05; **P<0.01; ***P<0.001. Unpaired t-test, two-tailed. Scale bar: 200 µm.

GPX4 interacts with Tcf/Lefs and occupies Wnt target gene promoters; depletion of GPX4 enhances Tcf/Lef binding to target promoters

The above genetic interaction analysis suggested that GPX4 inhibits Wnt/β-catenin signaling at the level of Tcf/Lef. In addition, a recent study has shown clearly that zebrafish Gpx4 preferentially accumulates in the nucleus from the 128- to 512-cell stages (Mendieta-Serrano et al., 2015). In cultured HeLa cells, GPX4 is distributed in the cytosol and nucleus (Fig. 7A). These findings suggest that GPX4/Gpx4 and Tcf/Lefs may interact with each other at some stages during embryogenesis, as well as in some cell types. To address this possibility, we first tested whether GPX4 and Tcf/Lefs interact with each other at endogenous levels. Co-immunoprecipitation (co-IP) assay indicated that endogenous GPX4 specifically retrieved endogenous TCF3 and TCF4 in HEK293T cells (Fig. 7B). Accordingly, endogenous GPX4 was detectable in Myc-tagged immunoprecipitates of four Tcf/Lef family members in reciprocal co-IP assays (Fig. 7B). Moreover, when Myc-tagged Tcf3 and Flag-tagged zebrafish Gpx4b were co-expressed in HEK293T cells, they were observed in the same complex (Fig. 7C). Next, a bimolecular fluorescence complementation (BiFC) assay, which was recently established to directly visualize the β-catenin-Tcf interaction in living cells (Ding et al., 2014), was used to assess the interaction of Gpx4b and Tcf in HeLa cells. The BiFC signals indicated that Gpx4b and Gpx4b-C interact with both Tcf3 and Tcf3ΔN in the nucleus, whereas they interact with Tcf3ΔNLS (lacking the nuclear localization signal) in the cytoplasm (Fig. 7D, Fig. S6A). These results indicated that Gpx4b and Gpx4b-C specifically and directly interact with Tcf3 in the nucleus and that the binding does not require the activation of Wnt signals. Moreover, BiFC signals derived from Gpx4b and β-catenin were barely detected, suggesting that they do not directly interact in living cells (Fig. S6B). As GPX4 overexpression inhibits VP16-Tcf3ΔN action, whereas GPX4 depletion synergistically enhances VP16-Tcf3ΔN action, we postulated that GPX4 inhibits VP16-Tcf3ΔN action by preventing Tcf3 binding to target gene promoters. To test this hypothesis, the mutant VP16-Tcf3(295-441) was used. VP16-Tcf3(295-441) lacks both activator β-catenin and repressor Groucho binding domains, and contains only the high-mobility group DNA-binding domain, which is sufficient to induce Wnt activity (Lu et al., 2015). Co-injection of *GPX4* or *gpx4b* mRNA with *VP16-Tcf3(295-441)* reduced VP16-Tcf3(295-441)-induced dorsalizing activity in zebrafish embryos (Fig. 7E,F). Accordingly, co-injection with *gpx4b* mRNA inhibited VP16-Tcf3 (295-441)-induced Wnt reporter activity (Fig. 7G). As GPX4 forms a complex with Tcf/Lefs, it is possible that GPX4 occupies a Wnt-regulated promoter. To examine this possibility, we carried out chromatin immunoprecipitation (ChIP)-PCR experiments using HEK293T cells to determine whether or not GPX4 occupies the promoters of Wnt target genes. ChIP assays showed that endogenous GPX4 associated with the promoters of Wnt target genes, such as *AXIN2*, *CCND1*, *DKK1* and *LEF1*, but not with those of *α-satellite* and *GAPDH* (Fig. 7H). As GPX4 and Gpx4b inhibited VP16-Tcf3(295-441)-induced Wnt activity and associated with the promoters of Wnt target genes, we speculated that GPX4 and Gpx4b may associate with Tcf/Lef proteins at target promoters and might act by hindering the association between Tcf/Lef proteins with the promoters of Wnt target genes. To test this hypothesis, we performed ChIP-qPCR experiments using GPX4-depleted HEK293T cells to determine the binding between Tcf/Lef

Development (2017) 144, 1687-1697 doi:10.1242/dev.144261

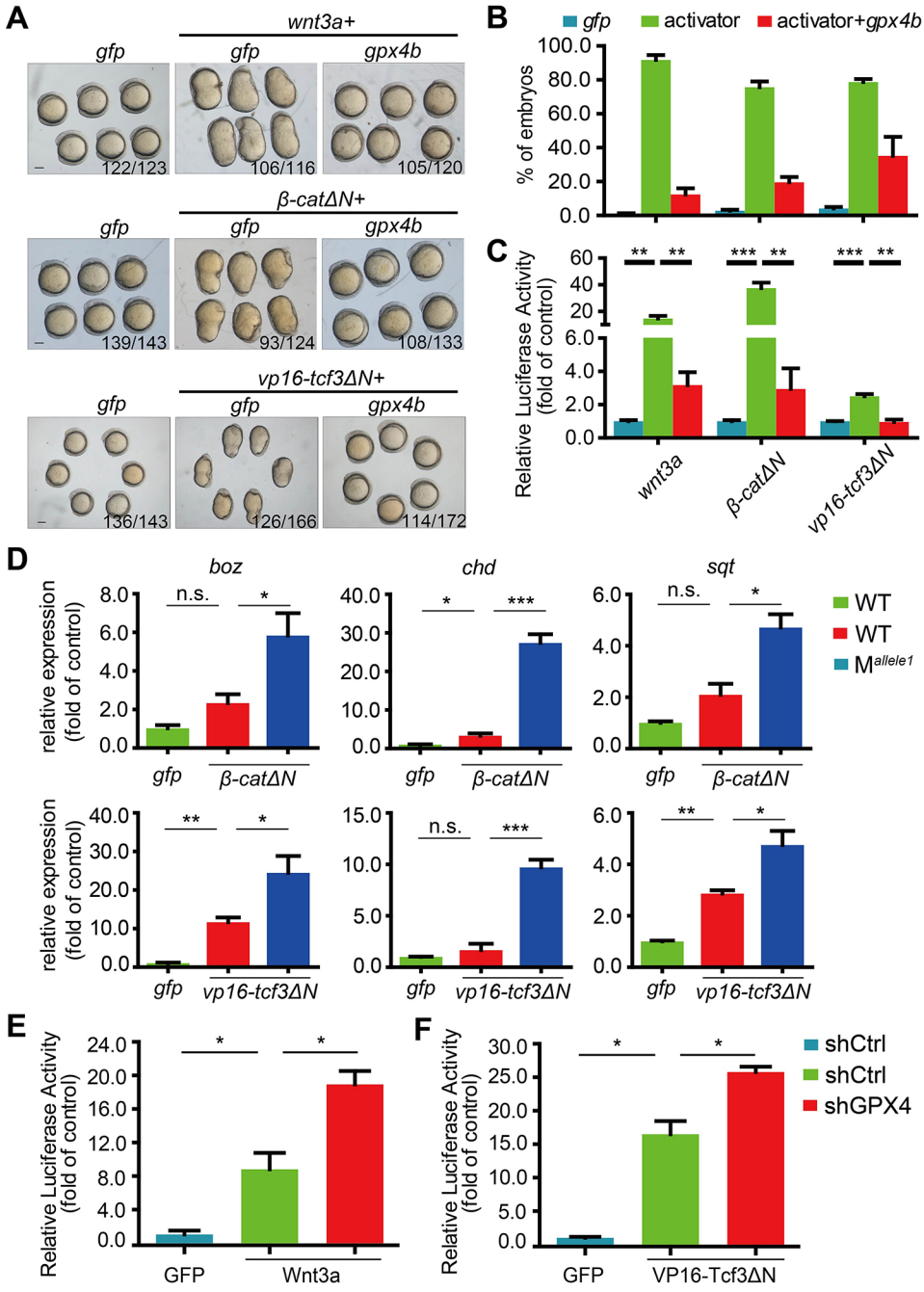

Fig. 5. GPX4/Gpx4b inhibits Wnt activity at the Tcf level. (A,B) Gpx4b inhibits the action of indicated Wnt activators *in vivo*. Representative images of embryos injected with 680 pg *gfp* mRNA, mRNA of each indicated Wnt activator (20 pg *wnt3a*, 50 pg *β-catΔN* and 80 pg *vp16-Tcf3ΔN*) and mRNA of each indicated Wnt activator plus 600 pg *gpx4b* mRNA at 12.5 hpf are shown in A. Quantitative results are shown in B. The frequency of embryos with the indicated phenotypes is shown in A. (C) Gpx4b inhibits Wnt activity induced by each indicated Wnt activator *in vivo*. Embryos were injected with TOPFlash reporter DNA with the indicated mRNAs (20 pg *wnt3a*, 50 pg *β-catΔN*, and 80 pg *vp16-Tcf3ΔN*). (D) Maternal loss of Gpx4b synergistically elevated *β-catΔN*- and *vp16-tcf3ΔN*-induced expression of *boz*, *chd* and *sqt* at 4.3 hpf. One-cell stage wild-type and maternal mutant embryos were injected with *gfp* (40 pg), *β-catΔN* (25 pg) or *vp16-tcf3ΔN* (40 pg) mRNA. The injected embryos were raised to 4.3 hpf and the expression levels of the indicated target genes were measured by qRT-PCR. (E,F) Knockdown of GPX4 synergistically enhances Wnt3a- and VP16-Tcf3ΔN-induced Wnt reporter activity. The indicated plasmid DNA (5 ng) was co-transfected with TOPFlash plasmid DNA into control or GPX4-knockdown HEK293T cells and the luciferase activity was measured. Results are from three independent experiments. Values are means±s.e.m. (n=3). *P<0.05; **P<0.01; ***P<0.001. Unpaired t-test, two-tailed. Scale bars: 200 µm.

proteins with the promoter sequences of Wnt target genes. As shown in Fig. 7I, GPX4 knockdown in HEK293T cells strengthened the association of TCF3 and TCF4, TCF4 alone, and LEF1 with the promoters of *AXIN2* and *DKK1*. Taken together, these data indicated that GPX4 is associated with Tcf/Lef proteins at the promoters of the Wnt target genes and prevents Tcf/Lef proteins from binding to their target gene promoters.

DISCUSSION

In this study, we report that depletion of maternal Gpx4b by CRISPR/Cas9-mediated knockout or MO-mediated knockdown promoted dorsal organizer formation in zebrafish embryos. Conversely, gain-of-function of *gpx4b* in zebrafish embryos resulted in ventralized embryos. A variety of data showed that GPX4/Gpx4b participates in Wnt/β-catenin signaling and that maternal Gpx4b affects embryonic dorsal organizer formation through regulation of this pathway. We observed upregulated expression of Wnt target genes and increased Wnt reporter activity after GPX4 and Gpx4b depletion *in vivo* and *in vitro*. Additionally, the expression areas of both maternal and zygotic Wnt target genes were largely expanded after Gpx4b depletion in zebrafish. Forced expression of *GPX4*/*gpx4b* impeded the development of the dorsal organizer and inhibited Wnt reporter activity. Genetic interaction analysis between GPX4 and an array of Wnt activators indicated that GPX4 acts at the level of Tcf/Lef. Importantly, we also showed that GPX4 interacts with Tcf/Lef family members and occupies Wnt target gene promoters, thereby preventing the association between Tcf/Lefs and their target promoters. The interaction between GPX4 and Tcf/Lefs results in the repression of Wnt/β-catenin target genes in the presence of Wnt signals. Intriguingly, catalytically inactivated

Development (2017) 144, 1687-1697 doi:10.1242/dev.144261

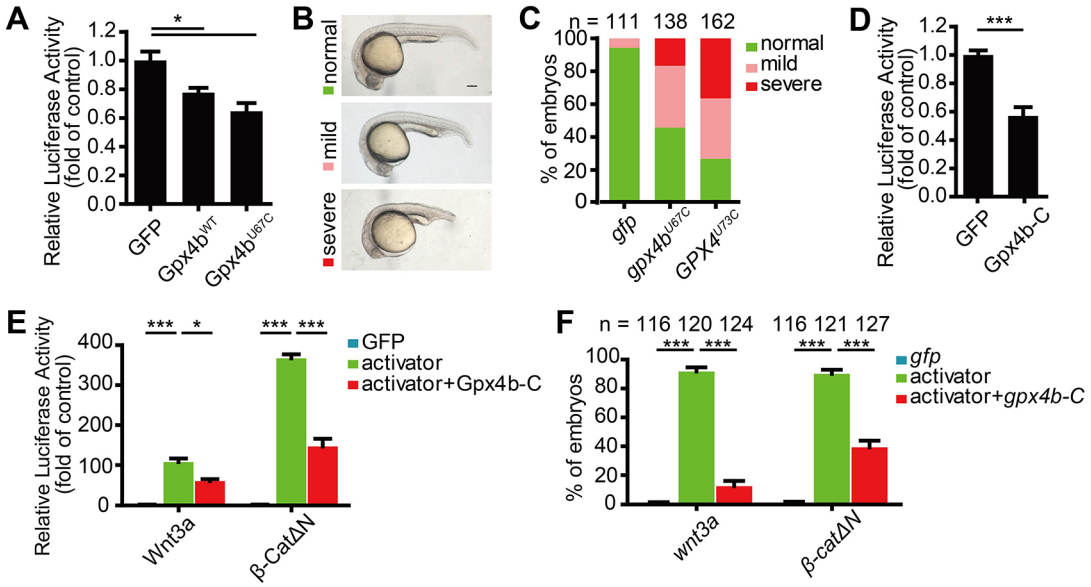

Fig. 6. Sec is dispensable for Wnt inhibition. (A) Gpx4b^{WT} and Gpx4b^{U67C} inhibit endogenous Wnt activity. The indicated plasmid DNA (200 ng) was co-transfected with TOPFlash plasmid DNA into HEK293T cells. (B) Classification of ventralized phenotypes at 24 hpf caused by forced expression of 600 pg *gpx4b*^{U67C} or *GPX4*^{U73C} mRNA. (C) Percentages of embryos in each category as shown in B. Results are from three independent experiments and the total embryo numbers are given at the top. (D) Gpx4b-C inhibits endogenous Wnt activity. The indicated plasmid DNA (600 ng) was co-transfected with TOPFlash plasmid DNA into HEK293T cells and the luciferase activity was measured. (E) Gpx4b-C inhibits Wnt3a and β-CatΔN activity *in vitro*. The indicated plasmid DNA (20 ng Wnt3a and 50 ng β-CatΔN) was co-transfected with TOPFlash plasmid DNA into HEK293T cells and the luciferase activity was measured. (F) Gpx4b-C inhibits Wnt3a and β-CatΔN action *in vivo*. Quantitative results are shown as in Fig. 5B. Embryos injected with 650 pg *gfp* mRNA, mRNA of each indicated Wnt activator (20 pg *wnt3a* and 50 pg *β-catΔN*) and mRNA of each indicated Wnt activator plus 600 pg *gpx4b-c* mRNA at 12.5 hpf. The total embryo numbers from three independent experiments are shown at the top of each bar. Values are mean±s.e.m. (*n*=3). **P*<0.05; ****P*<0.001. Unpaired *t*-test, two-tailed. Scale bar: 200 µm.

GPX4/Gpx4b also ventralized embryos and was sufficient to inhibit the Wnt/β-catenin signal, suggesting that the Sec residue is dispensable for Wnt inhibition. These findings suggested that GPX4 and Gpx4b are novel inhibitors of the Wnt/β-catenin pathway.

An interesting observation made in this study is that maternal Gpx4b regulates dorsal organizer formation in zebrafish embryos. Previous studies have reported that genetic ablation of GPX4 or targeted mutation of the active-site Sec in mice leads to embryonic lethality around E7.5, implying that the survival function of GPX4 is conferred by its peroxidase activity mediated through Sec (Imai et al., 2003; Ingold et al., 2015; Yant et al., 2003). By contrast, zygotic *gpx4b* mutant fish are viable, morphologically normal, and fertile. This is not surprising, as the zebrafish genome harbors two *gpx4* genes (*gpx4a* and *gpx4b*), which both have a Sec site. Another, Gpx4a can rescue *gpx4b* morphants. Thus, Gpx4a may partially compensate the genetic loss of function of Gpx4b. In addition, we cannot exclude the possibility that the presence of maternal Gpx4 protein may also have contributed to the rescue of the early developmental defect in zygotic *gpx4b* mutant embryos (Mendieta-Serrano et al., 2015). Intriguingly, M and MZ mutants and morphants all exhibited an enlarged dorsal organizer at 4.3 hpf and, yet, they showed distinct phenotypes at 24 or 26 hpf. M mutants showed a weakly dorsalized phenotype, while dorsalization was relatively stronger in morphants. Our results indicate that genetic loss of maternal Gpx4b but not *gpx4b* knockdown may induce the activation of a compensatory network in zebrafish embryos. The evidence includes the following observations: (1) both M mutants and morphants display robust elevation of Wnt signaling, although the strength of the dorsalized phenotype between them is largely different; (2) the transcript level of *gpx4a* is significantly upregulated in M mutant embryos but not in *gpx4b*-knockdown morphants at 4 hpf; and (3) Gpx4a and Gpx4b have a comparable ventralizing action. Similarly, Rossi et al. (2015) recently observed different phenotypes in *egfl7*$^{-/-}$ genetic mutants and Egfl7 morphants, and demonstrated that compensation mechanisms could be activated to buffer against deleterious mutations in zebrafish (Rossi et al., 2015). On the other hand, variable compensation may also contribute to penetrance and expressivity between intra- and inter-genetic lines. Recently, similar incomplete penetrance and variable expressivity were found in a high-throughput analysis of developmental phenotypes in mice that supported this view (Dickinson et al., 2016). Additionally, genetic knockout and MO-based knockdown have different effects: genetic knockout of *gpx4b* caused complete loss of Gpx4b protein, while the injected MO might be gradually diluted throughout embryonic development, with insufficient MO remaining to block the translation of zygotic *gpx4b* mRNA. As mentioned earlier, maternal Wnt promotes dorsal development whereas zygotic Wnt limits dorsal development. Gpx4b inhibits both maternal and zygotic Wnt/β-catenin activity. Thus, a possible explanation for the MZ mutant phenotype is that these two events likely cancel each other out on dorsoventral patterning. The similar dorsoventral patterning between MZ mutants and morphants before the onset of gastrulation and the distinct dorsoventral patterning between them after the onset of gastrulation support this view. This might underlie the different phenotypes observed in MZ mutants and morphants. In zebrafish, zygotic Wnt/β-catenin signaling is also involved in anteroposterior neuroectoderm patterning (Erter et al., 2001; Lekven et al., 2001). Although significantly increased zygotic Wnt activity was detected in the MZ *gpx4b* mutant embryos, no change in anteroposterior neural patterning was observed,

Development (2017) 144, 1687-1697 doi:10.1242/dev.144261

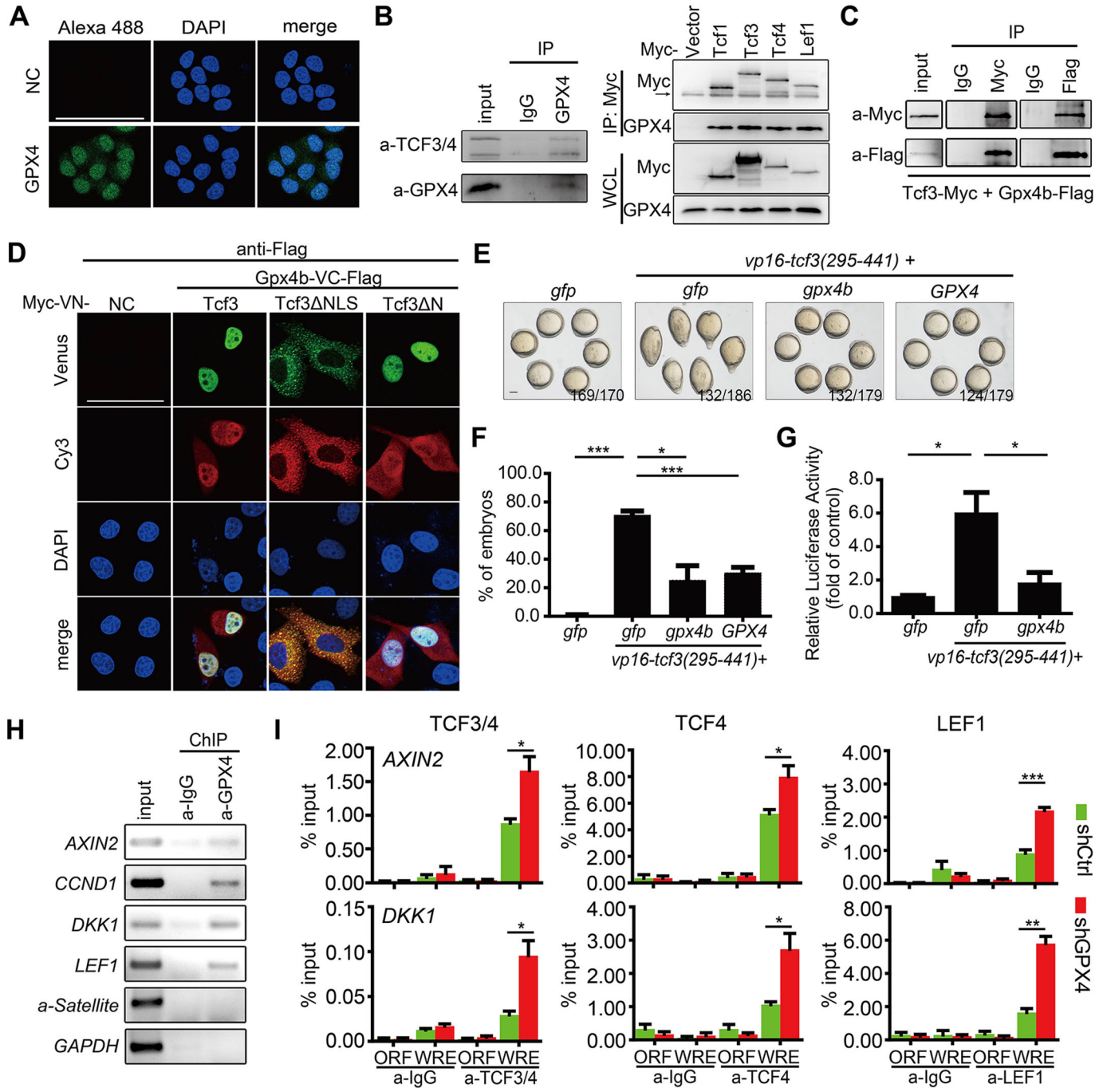

Fig. 7. GPX4/Gpx4b binds to and prevents Tcf/Lef binding to target promoters. (A) Distribution of endogenous GPX4 protein in HeLa cells, visualized by immunofluorescence (green) with an anti-GPX4 antibody. Nuclei (blue) were stained with DAPI. Scale bar: 75 µm. (B) Endogenous GPX4 interacts with Tcf/Lef members, as indicated by co-immunoprecipitaton. Left panel: GPX4 interacts with TCF3/4 in HEK293T cells. Right panel: four Myc-tagged Tcf/Lef members interact with endogenous GPX4 in HEK293T cells. The indicated proteins were immunoprecipitated or detected using appropriate antibodies. Vector, empty expressing plasmid with myc tag; WCL, whole-cell lysate; IP, immunoprecipitate; input, positive control; IgG, negative control; arrow, IgG heavy chain. (C) Exogenous Gpx4b interacts with Tcf3. Proteins were extracted from lysates of cells that co-expressed tagged Tcf3 and Gpx4b, immunoprecipitated and subjected to western blot analysis using the indicated antibodies. (D) Gpx4b interacts with each indicated form of Tcf3 in living cells, as indicated by BiFC assay. Flag-tagged Gpx4b-VC expression vector was co-transfected with the indicated forms of Tcf3-VN. Expression of Gpx4b detected by anti-Flag antibody immunostaining (red). NC, negative control. Scale bar: 50 µm. (E,F) Zebrafish Gpx4b and human GPX4 inhibit VP16-Tcf3(295-441) action *in vivo*. One-cell stage wild-type embryos were injected with indicated mRNAs [680 pg *gfp* mRNA alone or 80 pg *vp16-tcf3(295-441)* plus 600 pg *gfp*, *gpx4b* or *GPX4* mRNA]. Representative images of each group of injected embryos at 12.5 hpf are shown in E. Quantitative results of the indicated phenotypes are shown in F. The frequency of embryos with the indicated phenotypes is shown in E. Scale bar: 200 µm. (G) Gpx4b inhibits VP16-Tcf3(295-441)-induced activity *in vivo*. Embryos were injected with TOPFlash reporter DNA with the indicated mRNAs [680 pg *gfp* mRNA alone or 80 pg *vp16-tcf3(295-441)* plus 600 pg *gfp* or *gpx4b* mRNA]. (H) Endogenous GPX4 is associated with the promoters of the indicated direct Wnt target genes in HEK293T cells, as indicated by ChIP assay. *α-Satellite* and *GAPDH* promoters were used as negative controls. (I) Knockdown of GPX4 enhances the binding of TCF3/4, TCF4 alone and LEF1 to the *AXIN2* and *DKK1* promoters in HEK293T cells. Values are means±s.e.m. (n=3). *P<0.05; **P<0.01; ***P<0.001. Unpaired t-test, two-tailed.

Development (2017) 144, 1687-1697 doi:10.1242/dev.144261

indicating that there might be functional redundancy between Gpx4b and other Wnt/β-catenin inhibitors. Similar dorsoventral patterning and anteroposterior neural patterning has been recently observed in MZ mutant embryos of Ptk7, an inhibitor of Wnt/β-catenin (Hayes et al., 2013). In addition, the expression domains between *gpx4b* and *ptk7* during gastrulation and segmentation stages also overlapped. Similar phenotype in MZ mutant embryos suggests that other Wnt/β-catenin inhibitors may be functionally redundant with Gpx4b.

Another key finding in this study is that GPX4/Gpx4b inhibits Wnt/β-catenin signaling at the level of Tcf/Lef and prevents the binding of Tcf/Lefs to promoters of Wnt target genes. We provided multiple lines of evidence to support the conclusion. First, epistasis experiments in zebrafish embryos suggested that inhibition of the Wnt pathway is due to the inhibition of VP16-Tcf3ΔN. In addition, maternal loss of *gpx4b* in zebrafish embryos synergistically elevated expression of *vp16-tcf3ΔN*-induced maternal Wnt target genes. Likewise, depletion of GPX4 in cultured HEK293T cells synergistically augmented VP16-Tcf3ΔN-induced Wnt reporter activity. Second, co-IP assays confirmed that GPX4 and TCF3/4 are in the same complex under physiological conditions and that endogenous GPX4 interacts with four Myc-tagged Tcf/Lef family members. Importantly, BiFC signals derived from Gpx4b and Tcf3, Tcf3ΔN and Tcf3ΔNLS but not from Gpx4b-β-catenin were detected when these proteins were co-expressed in HeLa cells, suggesting that Gpx4b and Tcf3 do directly interact in living cells. Third, ChIP-PCR experiments showed that endogenous GPX4 occupies the promoters of *AXIN2*, *CCND1*, *DKK1* and *LEF1*. Fourth, GPX4/Gpx4b inhibited VP16-Tcf3(295-441)-induced activity. When GPX4 was depleted, the association of TCF3 and TCF4, TCF4 alone, and LEF1 with the promoters of *AXIN2* and *DKK1* was strengthened. These data strongly suggest that GPX4 and Gpx4b interact with Tcf/Lef proteins, occupy the promoters of Wnt target genes and prevent Tcf/Lef proteins from binding target gene promoters. It should be noted that Tcf3 has been shown to function primarily as a transcriptional repressor in various contexts (Dorsky et al., 2003; Kim et al., 2000; Wu et al., 2012; Yi et al., 2011). Our results indicate that GPX4 also binds to Tcf3 to inhibit its action. The physiological effect of the interaction between GPX4 and Tcf3 needs further investigation.

We demonstrated that GPX4 and Gpx4b Sec activation is not required for Wnt signaling inhibition. The evidence for this includes the following observations: (1) both Sec-to-Cys point mutants, as well as N-terminal and Sec-site deletion mutants, had similar Wnt inhibitory activity to wild-type GPX4 and Gpx4b in zebrafish embryos and cultured cells; (2) human and zebrafish Sec-to-Cys point mutants had a similar ventralizing action in zebrafish embryos; and (3) the N-terminal and Sec-site deletion mutant and the Tcf3, Tcf3ΔN and Tcf3ΔNLS produced BiFC signals when they were co-expressed in HeLa cells. It should be mentioned that although inactivation of Sec was sufficient to inhibit Wnt activity, we cannot exclude the possibility that GPX4 and Gpx4b might partially affect Wnt signaling indirectly. For example, depletion of GPX4 leads to increased cellular ROS, which activates multiple signaling pathways, including Wnt/β-catenin signaling (Funato et al., 2006, 2010; Kajla et al., 2012; Love et al., 2013; Rharass et al., 2014; Sandieson et al., 2014; Wen et al., 2012). Future studies are needed to elucidate such additional mechanisms. In addition, GPX4 might modulate other components of Wnt signaling: this needs to be investigated in the future.

In summary, we have characterized the phenotypes of *gpx4b*-deficient zebrafish embryos in detail. Our study reveals a novel function of the selenoprotein GPX4 as an inhibitor of canonical Wnt signaling that prevents the association of Tcf/Lef proteins with the promoters of Wnt target genes. The findings reported here will improve our understanding of the molecular mechanism of GPX4 and Gpx4b function at the cellular level and in embryonic development. Although the active-site Sec of GPX4 is dispensable for Wnt inhibition, selenium in the form of Sec is a prerequisite for GPX4 synthesis. Dietary selenium has been clearly shown to influence the translational efficiency of GPX4 in rats (Weiss Sachdev and Sunde, 2001). This raises an interesting issue about the relationships between dietary selenium, GPX4, Wnt/β-catenin signaling activity and even disease, providing scope for future research.

MATERIALS AND METHODS

Zebrafish strains

The wild-type zebrafish (*Danio rerio*) strain Tübingen was used in this study. The *gpx4b* knockout mutant strain was constructed using the CRISPR/Cas9 system (Chang et al., 2013). Embryos obtained by natural cross were kept in embryo-rearing solution at a standard 28.5°C, as described previously (Rong et al., 2014). Embryos were strictly staged according to standard methods (Kimmel et al., 1995). All experimental protocols were approved by and conducted in accordance with the Ethical Committee of Experimental Animal Care, Ocean University of China.

Cell culture and luciferase assays

HEK293T cells were purchased from ATCC. Cell culture, transfection and luciferase assays were performed as described previously (Feng et al., 2012). The *in vivo* luciferase assay was performed as reported previously (Rong et al., 2014). For further details, see the supplementary Materials and Methods.

Stable GPX4 knockdown cell line construction

The stable GPX4 knockdown cell line was established by lentiviral delivery of shRNA in the HEK293T cell line. The interference sequence (GTGGATGAAGATCCAACCC) was designed and provided by Sigma. For further details, see the supplementary Materials and Methods.

Capped mRNA synthesis, morpholino and microinjection

Capped mRNA was synthesized using the mMESSAGE mMACHINE Kit. To knock down *gpx4b*, a translation-blocking MO oligonucleotide targeting *gpx4b* was purchased and diluted as described previously (Rong et al., 2014). Diluted MO and/or mRNA were injected into one-cell stage zebrafish embryos. A GFP reporter plasmid containing the 5′-UTR and partial ORF (−27-114 bp) of zebrafish *gpx4b* was constructed and used to examine the efficiency of the MO.

Immunocytochemistry and BiFC

For immunocytochemistry, HeLa cells grown on a coverslip were fixed with 4% paraformaldehyde for 20 min at room temperature, followed by 0.2% Triton X-100 treatment for 5 min and blocking with 20% BSA. The cells were then incubated with corresponding primary and secondary antibodies along with DAPI for visualization of the nuclei.

Plasmids for BiFC assays were a gift from Dr Wei Wu (Ding et al., 2014). Zebrafish Gpx4b^{U67C} and Gpx4b-C were subcloned into the pCDNA3.1-Myc-VN vector and pCDNA3.1-Flag-VC vector. HeLa cells were transfected with the constructs and Venus fluorescent protein was selected as the reporter for complementation.

Fluorescence images were acquired with a Leica TCS SP8 confocal microscope.

Co-IP, western blotting and ChIP assay

Western blotting and Co-IP were performed mainly as described previously (Bai et al., 2014). ChIP assays were conducted using a ChIP assay kit (Millipore) according to the manufacturer's protocol. For further details, see the supplementary Materials and Methods.

Development (2017) 144, 1687-1697 doi:10.1242/dev.144261

Molecular cloning and plasmid construction

The full-length cDNA of zebrafish *gpx4a* and *gpx4b* and human *GPX4* with/without the 3'-UTR were amplified and cloned into the pCS2+ expression vector. For further details, see the supplementary Materials and Methods.

Chemicals, reagents and antibodies

All reagents were used strictly according to the instructions. The working concentration for each antibody was further adjusted according to the pilot experiment. Primers and sequence information are provided in Table S1. For further details, see the supplementary Materials and Methods.

RT-PCR and whole-mount *in situ* hybridization

RT-PCR and whole-mount *in situ* hybridization were performed mainly as described previously (Rong et al., 2014). For further details, see the supplementary Materials and Methods and Table S1 for primers.

Statistical analysis

Data are presented as the means±s.e.m. Differences among groups were analyzed using GraphPad Prism version 5.01 (San Diego, CA, USA). Statistical significance was accepted at $P<0.05$.

Acknowledgements

We are grateful to Dr Cunming Duan of the University of Michigan and to Dr Shaojun Du of the University of Maryland for critical suggestions. We thank Dr Wei Wu of Tsinghua University and Dr Ying Cao of Nanjing University for providing reagents. We thank Dr Hiroyasu Kamei (The University of Tokyo) for critical reading of this manuscript.

Competing interests

The authors declare no competing or financial interests.

Author contributions

X.R. designed and performed the experiments, analyzed the data, and wrote the manuscript; Y.Z., Y.L., B.Z., B.W., C.W., X.G. and P.T. performed the experiments; L.L., Y.L. and C.Z. provided analytical tools and reagents; and J.Z. supervised experimental design, data analysis and wrote the manuscript.

Funding

This work was supported by grants from the Major Science Programs of China [2011CB943800 to J.Z. and Y.Li], the National Natural Science Foundation of China-Shandong Joint Fund [U1406402 to J.Z.], and the National Natural Science Foundation of China [30972238 to J.Z., 31572261 to L.L. and 31601863 to X.R.]; by the Fundamental Research Funds for the Central Universities [201562028 to J.Z.], by the Scientific and Technological Innovation Project financially supported by Qingdao National Laboratory for Marine Science and Technology [2015ASKJ02 to J.Z.] and by AoShan talents program supported by Qingdao National Laboratory for Marine Science and Technology [2015ASTP-ES13 to C.Z.].

Supplementary information

Supplementary information available online at
http://dev.biologists.org/lookup/doi/10.1242/dev.144261.supplemental

References

Anastas, J. N. and Moon, R. T. (2013). WNT signalling pathways as therapeutic targets in cancer. *Nat. Rev. Cancer* **13**, 11-26.

Bai, Y., Tan, X., Zhang, H., Liu, C., Zhao, B., Li, Y., Lu, L., Liu, Y. and Zhou, J. (2014). Ror2 receptor mediates Wnt11 ligand signaling and affects convergence and extension movements in zebrafish. *J. Biol. Chem.* **289**, 20664-20676.

Baker, K. D., Ramel, M.-C. and Lekven, A. C. (2010). A direct role for Wnt8 in ventrolateral mesoderm patterning. *Dev. Dyn.* **239**, 2828-2836.

Bellipanni, G., Varga, M., Maegawa, S., Imai, Y., Kelly, C., Myers, A. P., Chu, F., Talbot, W. S. and Weinberg, E. S. (2006). Essential and opposing roles of zebrafish beta-catenins in the formation of dorsal axial structures and neurectoderm. *Development* **133**, 1299-1309.

Berry, M. J., Banu, L., Chen, Y. Y., Mandel, S. J., Kieffer, J. D., Harney, J. W. and Larsen, P. R. (1991). Recognition of UGA as a selenocysteine codon in type I deiodinase requires sequences in the 3′ untranslated region. *Nature* **353**, 273-276.

Brigelius-Flohé, R. and Maiorino, M. (2013). Glutathione peroxidases. *Biochim. Biophys. Acta* **1830**, 3289-3303.

Cadigan, K. M. and Waterman, M. L. (2012). TCF/LEFs and Wnt signaling in the nucleus. *Cold Spring Harb. Perspect. Biol.* **4**, a007906.

Chang, N., Sun, C., Gao, L., Zhu, D., Xu, X., Zhu, X., Xiong, J.-W. and Xi, J. J. (2013). Genome editing with RNA-guided Cas9 nuclease in zebrafish embryos. *Cell Res.* **23**, 465-472.

Clevers, H. and Nusse, R. (2012). Wnt/beta-catenin signaling and disease. *Cell* **149**, 1192-1205.

Dickinson, M. E., Flenniken, A. M., Ji, X., Teboul, L., Wong, M. D., White, J. K., Meehan, T. F., Weninger, W. J., Westerberg, H., Adissu, H. et al. (2016). High-throughput discovery of novel developmental phenotypes. *Nature* **537**, 508-514.

Ding, Y., Su, S., Tang, W., Zhang, X., Chen, S., Zhu, G., Liang, J., Wei, W., Guo, Y., Liu, L. et al. (2014). Enrichment of the beta-catenin-TCF complex at the S and G2 phases ensures cell survival and cell cycle progression. *J. Cell Sci.* **127**, 4833-4845.

Dixon, S. J., Lemberg, K. M., Lamprecht, M. R., Skouta, R., Zaitsev, E. M., Gleason, C. E., Patel, D. N., Bauer, A. J., Cantley, A. M., Yang, W. S. et al. (2012). Ferroptosis: an iron-dependent form of nonapoptotic cell death. *Cell* **149**, 1060-1072.

Dorsky, R. I., Itoh, M., Moon, R. T. and Chitnis, A. (2003). Two tcf3 genes cooperate to pattern the zebrafish brain. *Development* **130**, 1937-1947.

Erter, C. E., Wilm, T. P., Basler, N., Wright, C. V. and Solnica-Krezel, L. (2001). Wnt8 is required in lateral mesendodermal precursors for neural posteriorization in vivo. *Development* **128**, 3571-3583.

Feng, Q., Zou, X., Lu, L., Li, Y., Liu, Y., Zhou, J. and Duan, C. (2012). The stress-response gene redd1 regulates dorsoventral patterning by antagonizing Wnt/beta-catenin activity in zebrafish. *PLoS ONE* **7**, e52674.

Friedmann Angeli, J. P., Schneider, M., Proneth, B., Tyurina, Y. Y., Tyurin, V. A., Hammond, V. J., Herbach, N., Aichler, M., Walch, A., Eggenhofer, E. et al. (2014). Inactivation of the ferroptosis regulator Gpx4 triggers acute renal failure in mice. *Nat. Cell Biol.* **16**, 1180-1191.

Funato, Y., Michiue, T., Asashima, M. and Miki, H. (2006). The thioredoxin-related redox-regulating protein nucleoredoxin inhibits Wnt-beta-catenin signalling through dishevelled. *Nat. Cell Biol.* **8**, 501-508.

Funato, Y., Terabayashi, T., Sakamoto, R., Okuzaki, D., Ichise, H., Nojima, H., Yoshida, N. and Miki, H. (2010). Nucleoredoxin sustains Wnt/beta-catenin signaling by retaining a pool of inactive dishevelled protein. *Curr. Biol.* **20**, 1945-1952.

Hatfield, D. L., Tsuji, P. A., Carlson, B. A. and Gladyshev, V. N. (2014). Selenium and selenocysteine: roles in cancer, health, and development. *Trends Biochem. Sci.* **39**, 112-120.

Hayes, M., Naito, M., Daulat, A., Angers, S. and Ciruna, B. (2013). Ptk7 promotes non-canonical Wnt/PCP-mediated morphogenesis and inhibits Wnt/beta-catenin-dependent cell fate decisions during vertebrate development. *Development* **140**, 1807-1818.

Hikasa, H. and Sokol, S. Y. (2013). Wnt signaling in vertebrate axis specification. *Cold Spring Harb. Perspect. Biol.* **5**, a007955.

Hu, M., Bai, Y., Zhang, C., Liu, F., Cui, Z., Chen, J. and Peng, J. (2016). Liver-enriched gene 1, a glycosylated secretory protein, binds to FGFR and mediates an anti-stress pathway to protect liver development in zebrafish. *PLoS Genet.* **12**, e1005881.

Imai, H., Hirao, F., Sakamoto, T., Sekine, K., Mizukura, Y., Saito, M., Kitamoto, T., Hayasaka, M., Hanaoka, K. and Nakagawa, Y. (2003). Early embryonic lethality caused by targeted disruption of the mouse PHGPx gene. *Biochem. Biophys. Res. Commun.* **305**, 278-286.

Ingold, I., Aichler, M., Yefremova, E., Roveri, A., Buday, K., Doll, S., Tasdemir, A., Hoffard, N., Wurst, W., Walch, A. et al. (2015). Expression of a catalytically inactive mutant form of glutathione peroxidase 4 (Gpx4) confers a dominant-negative effect in male fertility. *J. Biol. Chem.* **290**, 14668-14678.

Kajla, S., Mondol, A. S., Nagasawa, A., Zhang, Y., Kato, M., Matsuno, K., Yabe-Nishimura, C. and Kamata, T. (2012). A crucial role for Nox 1 in redox-dependent regulation of Wnt-beta-catenin signaling. *FASEB J.* **26**, 2049-2059.

Kim, C.-H., Oda, T., Itoh, M., Jiang, D., Artinger, K. B., Chandrasekharappa, S. C., Driever, W. and Chitnis, A. B. (2000). Repressor activity of Headless/Tcf3 is essential for vertebrate head formation. *Nature* **407**, 913-916.

Kimmel, C. B., Ballard, W. W., Kimmel, S. R., Ullmann, B. and Schilling, T. F. (1995). Stages of embryonic development of the zebrafish. *Dev. Dyn.* **203**, 253-310.

Langdon, Y. G. and Mullins, M. C. (2011). Maternal and zygotic control of zebrafish dorsoventral axial patterning. *Annu. Rev. Genet.* **45**, 357-377.

Lekven, A. C., Thorpe, C. J., Waxman, J. S. and Moon, R. T. (2001). Zebrafish wnt8 encodes two wnt8 proteins on a bicistronic transcript and is required for mesoderm and neurectoderm patterning. *Dev. Cell* **1**, 103-114.

Love, N. R., Chen, Y., Ishibashi, S., Kritsiligkou, P., Lea, R., Koh, Y., Gallop, J. L., Dorey, K. and Amaya, E. (2013). Amputation-induced reactive oxygen species are required for successful Xenopus tadpole tail regeneration. *Nat. Cell Biol.* **15**, 222-228.

Lu, L., Gao, Y., Zhang, Z., Cao, Q., Zhang, X., Zou, J. and Cao, Y. (2015). Kdm2a/b lysine demethylases regulate canonical Wnt signaling by modulating the stability of nuclear beta-catenin. *Dev. Cell* **33**, 660-674.

MacDonald, B. T., Tamai, K. and He, X. (2009). Wnt/beta-catenin signaling: components, mechanisms, and diseases. *Dev. Cell* **17**, 9-26.

Mendieta-Serrano, M. A., Schnabel, D., Lomeli, H. and Salas-Vidal, E. (2015). Spatial and temporal expression of zebrafish glutathione peroxidase 4 a and b genes during early embryo development. *Gene Expr. Patterns* **19**, 98-107.

Mullins, M. C., Hammerschmidt, M., Kane, D. A., Odenthal, J., Brand, M., van Eeden, F. J., Furutani-Seiki, M., Granato, M., Haffter, P., Heisenberg, C. P. et al. (1996). Genes establishing dorsoventral pattern formation in the zebrafish embryo: the ventral specifying genes. *Development* **123**, 81-93.

Petersen, C. P. and Reddien, P. W. (2009). Wnt signaling and the polarity of the primary body axis. *Cell* **139**, 1056-1068.

Ramel, M.-C., Buckles, G. R., Baker, K. D. and Lekven, A. C. (2005). WNT8 and BMP2B co-regulate non-axial mesoderm patterning during zebrafish gastrulation. *Dev. Biol.* **287**, 237-248.

Rharass, T., Lemcke, H., Lantow, M., Kuznetsov, S. A., Weiss, D. G. and Panáková, D. (2014). Ca2+-mediated mitochondrial reactive oxygen species metabolism augments Wnt/beta-catenin pathway activation to facilitate cell differentiation. *J. Biol. Chem.* **289**, 27937-27951.

Rong, X., Chen, C., Zhou, P., Zhou, Y., Li, Y., Lu, L., Liu, Y., Zhou, J. and Duan, C. (2014). R-spondin 3 regulates dorsoventral and anteroposterior patterning by antagonizing Wnt/beta-catenin signaling in zebrafish embryos. *PLoS ONE* **9**, e99514.

Rossi, A., Kontarakis, Z., Gerri, C., Nolte, H., Hölper, S., Krüger, M. and Stainier, D. Y. R. (2015). Genetic compensation induced by deleterious mutations but not gene knockdowns. *Nature* **524**, 230-233.

Sandieson, L., Hwang, J. T. K. and Kelly, G. M. (2014). Redox regulation of canonical Wnt signaling affects extraembryonic endoderm formation. *Stem Cells Dev.* **23**, 1037-1049.

Schneider, S., Steinbeisser, H., Warga, R. M. and Hausen, P. (1996). Beta-catenin translocation into nuclei demarcates the dorsalizing centers in frog and fish embryos. *Mech. Dev.* **57**, 191-198.

Seiler, A., Schneider, M., Förster, H., Roth, S., Wirth, E. K., Culmsee, C., Plesnila, N., Kremmer, E., Radmark, O., Wurst, W. et al. (2008). Glutathione peroxidase 4 senses and translates oxidative stress into 12/15-lipoxygenase dependent- and AIF-mediated cell death. *Cell Metab.* **8**, 237-248.

Stamos, J. L. and Weis, W. I. (2013). The beta-catenin destruction complex. *Cold Spring Harb. Perspect. Biol.* **5**, a007898.

Thisse, C., Degrave, A., Kryukov, G. V., Gladyshev, V. N., Obrecht-Pflumio, S., Krol, A., Thisse, B. and Lescure, A. (2003). Spatial and temporal expression patterns of selenoprotein genes during embryogenesis in zebrafish. *Gene Expr. Patterns* **3**, 525-532.

Weiss Sachdev, S. and Sunde, R. A. (2001). Selenium regulation of transcript abundance and translational efficiency of glutathione peroxidase-1 and -4 in rat liver. *Biochem. J.* **357**, 851-858.

Wen, J. W. H., Hwang, J. T. K. and Kelly, G. M. (2012). Reactive oxygen species and Wnt signalling crosstalk patterns mouse extraembryonic endoderm. *Cell. Signal.* **24**, 2337-2348.

Wu, C.-I., Hoffman, J. A., Shy, B. R., Ford, E. M., Fuchs, E., Nguyen, H. and Merrill, B. J. (2012). Function of Wnt/beta-catenin in counteracting Tcf3 repression through the Tcf3-beta-catenin interaction. *Development* **139**, 2118-2129.

Yang, W. S., SriRamaratnam, R., Welsch, M. E., Shimada, K., Skouta, R., Viswanathan, V. S., Cheah, J. H., Clemons, P. A., Shamji, A. F., Clish, C. B. et al. (2014). Regulation of ferroptotic cancer cell death by GPX4. *Cell* **156**, 317-331.

Yant, L. J., Ran, Q., Rao, L., Van Remmen, H., Shibatani, T., Belter, J. G., Motta, L., Richardson, A. and Prolla, T. A. (2003). The selenoprotein GPX4 is essential for mouse development and protects from radiation and oxidative damage insults. *Free Radic. Biol. Med.* **34**, 496-502.

Yi, F., Pereira, L., Hoffman, J. A., Shy, B. R., Yuen, C. M., Liu, D. R. and Merrill, B. J. (2011). Opposing effects of Tcf3 and Tcf1 control Wnt stimulation of embryonic stem cell self-renewal. *Nat. Cell Biol.* **13**, 762-770.